Partial oxidation of methane to syngas over calcined Ni–Mg/Al layered double hydroxides

Kyung Moo Lee and Wha Young Lee *

School of Chemical Engineering, Seoul National University, Shillim-dong, Kwanak-ku, Seoul 151-742, Korea

Received 8 April 2002; accepted 30 May 2002

The catalytic partial oxidation of CH_4 to syngas was carried out over an Ni–Mg/Al mixed-oxide catalyst prepared from layered double hydroxide-type precursors. The catalysts were characterized by XRD, TPR, UV-DRS, XRF, BET and CHNS analysis. The effects of the catalyst composition and the calcination temperature on the catalytic performance and the extent of catalyst deactivation were investigated. Ni–Mg/Al oxide catalysts converted CH_4 into syngas efficiently with high selectivity. The catalyst performance was strongly related to the Ni particle size and the calcination temperature. The catalysts that were calcined at higher temperature exhibited a better catalytic performance. In conclusion, the $NiAl_2O_4$ spinel phase had a positive effect on the stability of the catalyst.

KEY WORDS: partial oxidation of methane; hydrotalcite; layered double hydroxide; nickel aluminate; particle size; deactivation.

1. Introduction

In recent years, the partial oxidation of methane to syngas has been extensively investigated. This process is mildly exothermic and advantageous over the conventional highly endothermic steam-reforming process. Moreover, it can produce syngas with an H_2/CO ratio of 2, which makes it suitable for methanol synthesis and the Fisher–Tropsch process [1].

A number of catalysts, including first-row transition metals (Ni, Co, Fe) and the noble metals (Rh, Pt, Ru, Ir), have been adapted to the partial oxidation of methane [2–5]. Among the catalysts studied, Rh was reported to be the most active and stable catalyst. However, because of the high cost of Rh and other noble metal catalysts, Ni appears to be more promising. Ni-based catalysts have been intensively studied due to their low cost. However, the main disadvantage of Ni catalysts is their rapid deactivation due to carbon deposition. Nevertheless, high dispersion of Ni metal over the catalyst or the use of some additives can reduce this [6].

The layered double hydroxides (LDHs) with the hydrotalcite structure are interesting materials as precursors for mixed-oxide catalysts [7]. LDHs consist of positively-charged hydroxide layers, charge-compensating anions and water molecules. These compounds can be easily converted into well-mixed oxides *via* the calcination procedure.

In this study, the partial oxidation of methane to syngas was carried out over Ni–Mg/Al mixed-oxide catalysts prepared from LDH precursors in a continuous-flow fixed-bed reactor. The effects of the catalyst composition and the calcination temperature on the catalyst performance and catalyst deactivation were intensively investigated. Ni–Mg/Al mixed-oxide catalysts were characterized by TPR, XRD, UV-DRS, BET and elemental analysis.

2. Experimental

2.1. Catalyst preparation

The Ni–Mg/Al LDHs were prepared by a coprecipitation method. A solution of $Ni(NO_3)_2{\cdot}6H_2O$, $Mg(NO_3)_2{\cdot}6H_2O$ and $Al(NO_3)_2{\cdot}9H_2O$ in distilled water was slowly added to a solution of NaOH and Na_2CO_3 in distilled water under vigorous stirring. The atomic ratio of the Mg, Al and Ni precursors was adjusted in order to synthesize the catalysts with 20 wt% of Ni. Catalysts with Mg/Al ratios of 0, 0.5, 2, 5 and ∞ were prepared. The pH was adjusted to 10 by adding NaOH solution. The mixing step was carried out for 3 h and the solution was then aged at 343 K for 16 h. The precipitate was then filtered and washed thoroughly with distilled water. This was followed by drying at 393 K for 24 h. Table 1 shows the properties of the dried Ni–Mg/Al LDHs.

The Ni–Mg/Al mixed-oxide catalysts were obtained by calcining the dried Ni–Mg/Al LDHs for 12 h. The calcination temperature was in the range of 623~1073 K. The Ni–Mg/Al mixed-oxide catalysts were denoted as NiHT(x)c(y), where x represents the Mg/Al ratio of the catalysts and y represents the calcination temperature (K). For example, NiHT(2)c(1073) refers to the catalyst with an Mg/Al ratio of 2 and where the calcination temperature was 1073 K.

* To whom correspondence should be addressed.
E-mail: wyl@snu.ac.kr

1011-372X/02/1000-0065/0

Table 1
Compositions and lattice parameters of the dried Ni–Mg/Al LDHs.

Catalyst	Ni content [a] (wt%)	Mg/Al [a] (atomic ratio)	Crystal size (nm) [b]	Lattice parameter c (Å) [b]	Lattice parameter a (Å) [b]
NiHT(0)	21.25	0	4.55	23.35	2.92
NiHT(0.5)	21.06	0.51	6.09	23.73	3.01
NiHT(2)	20.48	1.98	13.31	23.77	3.06
NiHT(5)	20.06	4.85	5.72	24.60	3.09
NiHT(∞)	23.52	∞	3.34	28.15	3.14

[a] Data from XRF analysis.
[b] Data calculated from XRD results.

2.2. Catalyst characterization

The catalysts were characterized by temperature programmed reduction (TPR), ultraviolet diffuse reflectance spectroscopy (UV-DRS), X-ray diffraction (XRD), BET, XRF and CHNS analysis.

The TPR measurements were carried out in a conventional flow system with a moisture trap connected to a TCD at temperatures ranging from room temperature to 1173 K at a heating rate of 10 K/min. The flow rate of the reducing gas was $H_2 = 2$ ml/min and $N_2 = 20$ ml/min for each 0.1 g of catalyst. The structure and crystallinity of the Ni–Mg/Al LDHs and Ni–Mg/Al mixed-oxide catalysts were confirmed by XRD (Rigaku, D/MAX-3C). The metallic states of the Ni species were confirmed by UV-DRS (Perkin-Elmer, Ramda-20 spectrometer) in the range 200–1000 nm. The specific surface area of the catalyst was measured by the BET method using an ASAP 2010. The amount of coke deposition on the catalysts during the reaction was measured by elemental analysis.

2.3. Partial oxidation of CH_4

The partial oxidation of methane to syngas was carried out in a continuous-flow fixed-bed reactor at atmospheric pressure. The Ni–Mg/Al mixed oxide catalyst (100 mg) was charged in a tubular quartz reactor and activated in a stream of hydrogen (10 ml/min) and nitrogen carrier gas (10 ml/min) at 1073 K for 1 h. After cooling to the reaction temperature (973 K), CH_4 and O_3 were then fed into the reactor together with the N_2 carrier gas. The feed ratio of the CH_4/O_2 was maintained at a stoichiometric ratio of 2. The products were analyzed by TCD in a GC using Ar as the carrier gas. Carbosphere (60/80 mesh) was used as the column material.

3. Results and discussion

3.1. XRD analysis

Figure 1 shows the XRD patterns of the Ni–Mg/Al LDHs. All the synthesized Ni–Mg/Al LDHs showed the typical peaks for the hydrotalcite structure except for NiHT(∞). In this case, an $Mg(OH)_2$–$Ni(OH)_3$ mixed-hydroxide structure was formed instead. In addition to the hydrotalcite phase, a bohemite aluminum hydroxide phase was observed in the case of NiHT(0). Kruissink *et al.* [8] reported that a single-phase layer structure exists only for $x_{Ni} > 0.5$. Below this limit, a bohemite phase is observed. Figure 2 shows the XRD patterns of the Ni–Mg/Al mixed-oxide catalysts obtained by calcination at 1073 K. NiO and $NiAl_2O_4$ (spinel) phases were formed with the collapse of the original layered structures. NiHT(0)c(1073) showed the characteristic blue color of pure $NiAl_2O_4$. The XRD pattern confirmed the presence of $NiAl_2O_4$. The peaks representing the $NiAl_2O_4$ phase decreased with the increasing Mg/Al ratio, indicating that the thermal stability of the Ni–Mg/Al LDHs increased with the increasing Mg/Al ratio. Table 2 summarizes the data from XRD analysis. It has been reported that the formation of the LDHs structure shows an optimum M^{2+}/M^{3+} ratio of approximately 3. The mean particle sizes of the LDHs in table 1 and the BET surface areas in table 2 supported the above result. Among the catalysts, NiHT(5)c(1073) was found to have the smallest NiO particle size.

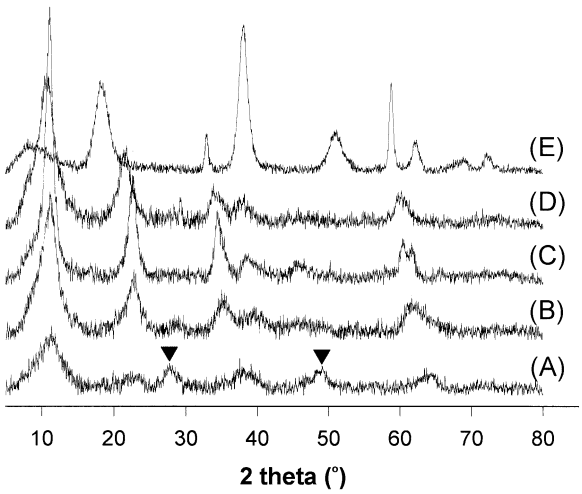

Figure 1. XRD patterns of the dried Ni–Mg/Al LDHs: (A) NiHT(0), (B) NiHT(0.5), (C) NiHT(2), (D) NiHT(5), (E) NiHT(∞): ▼ = bohemite phase.

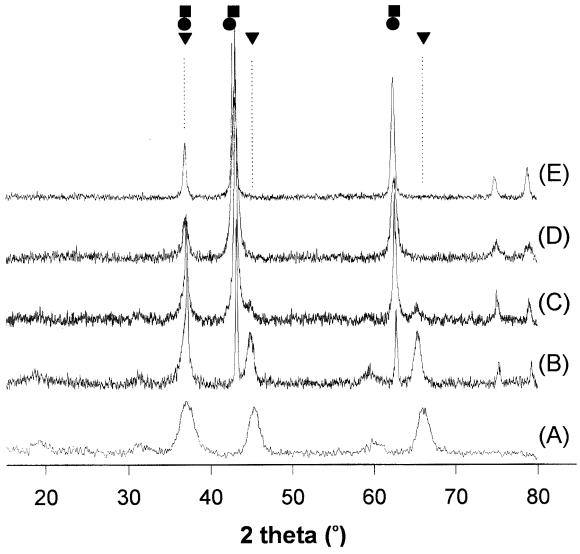

Figure 2. XRD patterns of the Ni–Mg/Al oxide catalysts calcined at 1073 K: (A) NiHT(0), (B) NiHT(0.5), (C) NiHT(2), (D) NiHT(5), (E) NiHT(∞): ● = MgO phase, ■ = NiO phase, ▼ = $NiAl_2O_4$ phase.

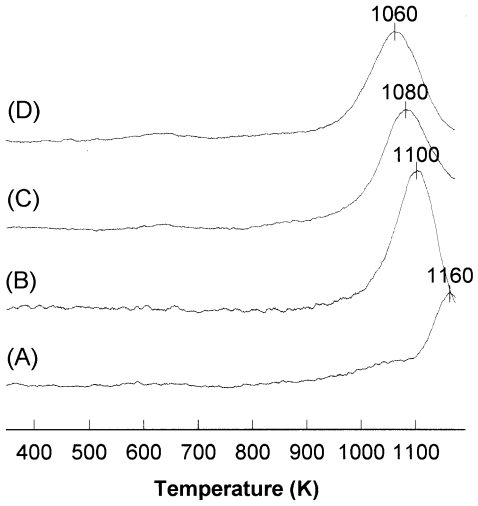

Figure 3. TPR profiles of the Ni–Mg/Al oxide catalysts calcined at 1073 K: (A) NiHT(0), (B) NiHT(0.5), (C) NiHT(2), (D) NiHT(5).

NiHT(0)c(1073) had $NiAl_2O_4$ peaks only, and the particle size of the $NiAl_2O_4$ was approximately 10 nm.

3.2. Temperature-programmed reduction

The TPR measurements were carried out in order to investigate the behavior of nickel metal in the reduction reactions. Figure 3 shows the reduction peaks of the Ni–Mg/Al oxide catalysts calcined at 1073 K. A broad peak was observed between 900 K and 1200 K for all samples. A much weaker peak between 600 K and 700 K, representing the reduction peak for NiO, was found in samples with a high Mg/Al ratio. However, NiHT(∞)c(1073) (not shown) showed only a weak reduction peak at low temperature. At the calcination temperature of 1073 K, a complete solid solution of NiO in MgO for the NiO–MgO catalyst is to be expected [9], and its reduction peak may show up at over 1173 K [10]. Therefore, the NiHT(∞)c(1073) catalyst is expected to have only a small amount of Ni metallic species under the pre-reduction conditions used in this study. The higher-temperature reduction peaks are attributed to $NiAl_2O_4$. Previous XRD analysis showed that there was no characteristic peak other than that of the NiO phase in the catalysts with a high Mg/Al ratio and the intensities of the NiO reduction peaks were significantly smaller than expected. This suggests that an amorphous NiA_2O_4 phase, which cannot be detected by XRD, exists near the NiO phase and hinders the reduction of the NiO phase. According to previous studies, the presence of Al ions in or around NiO particles may stabilize the NiO against sintering. However, it makes the reduction of the NiO phase more difficult [11–13]. The higher-temperature peaks shifted to a lower temperature with increasing Mg/Al ratio. This can be attributed to a decrease in the amount of $NiAl_2O_4$ phase due to the lower Al content.

3.3. UV-DRS

In order to confirm the identity of the nickel species and the formation of $NiAl_2O_4$, UV-DRS analysis was conducted. Figure 4 shows the results. All the catalysts showed three kinds of bands. According to literature on UV-DRS measurements of nickel oxide catalysts [14], the absorption bands of the octahedral Ni(II) ions in the NiO lattice were found at ~27 000, ~14 000 and ~13 000 cm^{-1}, together with an octahedral NiO(II) band in the Al_2O_3 lattice at ~24 000 cm^{-1}. The absorption bands of the tetrahedral Ni(II) ions in the Al_2O_3

Table 2
XRD and BET results of Ni–Mg/Al oxide catalysts calcined at 1073 K.

Catalyst	Observed phase	NiO particle size (nm)	MgO particle size (nm)	BET surface area (m^2/g)
NiHT(0)(1073)	$NiAl_2O_4$	–	–	100
NiHT(0.5)(1073)	NiO, $NiAl_2O_4$	68.4	54.7	113
NiHT(2)(1073)	NiO, $NiAl_2O_4$	48.8	44.3	137
NiHT(5)(1073)	NiO, MgO	20.1	19.8	117
NiHT(∞)(1073)	NiO, MgO	40.7	42.2	40

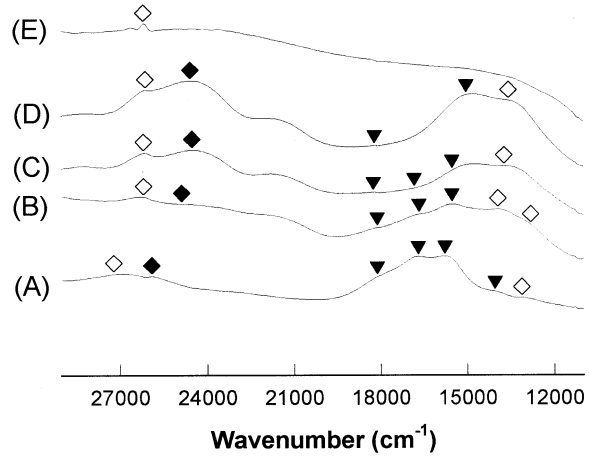

Figure 4. UV-DRS profiles of the Ni–Mg/Al oxide catalysts calcined at 1073 K: (A) NiHT(0), (B) NiHT(0.5), (C) NiHT(2), (D) NiHT(5), (E) NiHT(∞): ◇ = octahedral Ni^{2+} in NiO lattice, ◆ = octahedral Ni^{2+} in Al_2O_3 lattice, ▼ = tetrahedral Ni^{2+} in Al_2O_3.

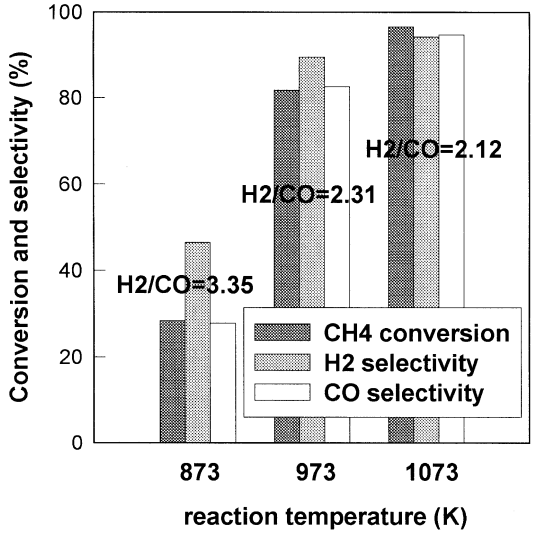

Figure 5. Catalytic activity of the NiHT(5)c(1073) for the partial oxidation of CH_4 with respect to reaction temperature ($CH_4/O_2 = 2$, GHSV = 13 500).

lattice were found at ~18 000, 16 700 and ~15 500 cm^{-1}. According to our XRD results, NiHT(0)c(1073) contained a single phase of $NiAl_2O_4$ and its UV-DRS result also showed spectra typical of pure $NiAl_2O_4$. The bands at 27 000 and 14 000 cm^{-1}, which represent octahedral Ni(II) ions in the NiO lattice, were not distinct in NiHT(0)c(1073). However, they became evident with increasing Mg/Al ratio. The absorption bands in the range of 16 000–18 000 cm^{-1} are typical of $NiAl_2O_4$. Considering that all the other catalysts showed these characteristic bands, it can be concluded that $NiAl_2O_4$ local orders exist, as suggested from the TPR results. These $NiAl_2O_4$ local orders were observed even in the samples calcined at low temperature (573 K). It is likely that the easy formation of the $NiAl_2O_4$ phase, in the calcined Ni–Mg/Al LDHs, is due to the structural characteristic of the LDHs that Ni species are mixed homogeneously with the Mg, Al species.

3.4. Partial oxidation of CH_4

The partial oxidation of CH_4 generally requires a high reaction temperature. This is due to the high dissociation energy of the CH_3–H bond and the fact that the undesirable total combustion reaction to CO_2 is thermodynamically favorable at lower temperatures. Figure 5 shows the catalytic activity of the NiHT(5)c(1073) catalyst for the partial oxidation of CH_4 as a function of reaction temperature. As the reaction temperature increased, the conversion of CH_4 and the selectivity for H_2 and CO increased simultaneously. At 873 K, the H_2/CO ratio was 3.35, which means that the total combustion to CO_2 and H_2O followed by a steam-reforming reaction ($H_2/CO = 4$) occurred dominantly. The conversion of O_2 was almost 100% in the reactions over 973 K. A large increase in the catalytic activity was observed at 973 K. Jin *et al.* [15] investigated CH_4 dissociation over Ni catalysts using the TPRS method and reported that the dissociation rate of CH_4 increased rapidly at 973–1023 K, which supports the above enhanced activity at temperatures above 973 K. At 1073 K, the conversion of CH_4 and selectivity for H_2 and CO after a 10 h reaction were 96.5, 95 and 94%, respectively.

Figure 6 shows the catalytic activities of the calcined LDHs after a 10 h reaction at 973 K. With the exception of NiHT(∞)c(1073), all samples exhibited similar activities. As mentioned above, NiHT(∞)c(1073) had a small amount of reducible Ni species in contrast to the other catalysts, which had NiO and $NiAl_2O_4$ phases reducible under 1073 K. Therefore, the active sites in

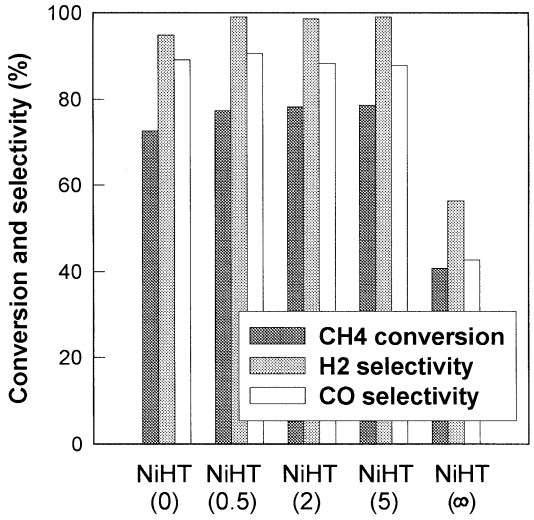

Figure 6. Catalytic activity of the Ni–Mg/Al oxide catalysts for the partial oxidation of CH_4 ($CH_4/O_2 = 2$, GHSV = 13 500, reaction temperature = 973 K).

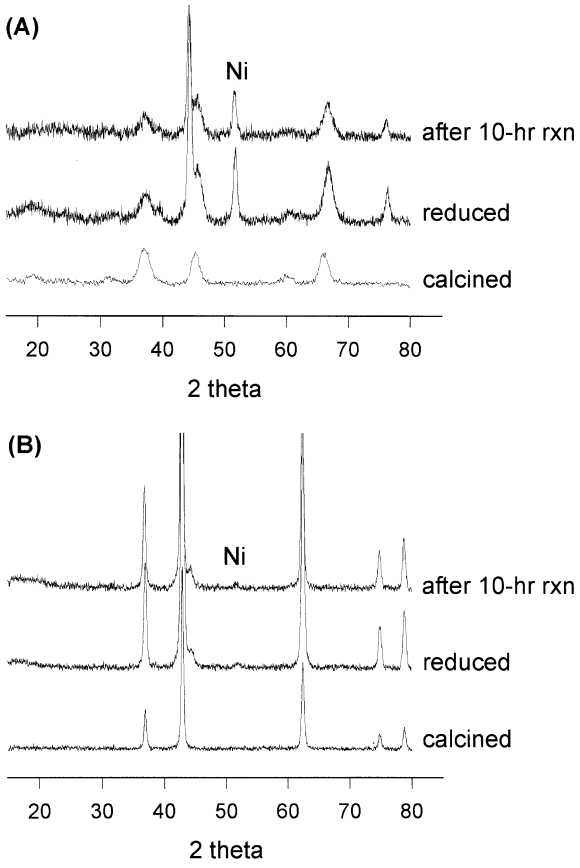

Figure 7. XRD patterns of the reduced and reacted catalysts: (A) NiHT(0)c(1073), (B) NiHT(∞)c(1073).

NiHT(∞)c(1073) appear to be associated with this small amount of Ni reducible under 1073 K, which was quickly deactivated. Figure 7 shows the XRD patterns of the reduced and used catalysts. NiHT(0)c(1073) showed the distinct peaks for metallic Ni species. The $NiAl_2O_4$ phase was still present in the material after reduction, as reported previously [16], and all the above peaks were found after a 10 h reaction. However, in the case of NiHT(∞)c(1073), only trace amounts of metallic Ni were found after the reduction, which suggests the low activity of NiHT(∞)c(1073).

Table 3 summarizes the degree of deactivation and the carbon content of the used catalysts. The deactivation rate showed a strong relationship to the carbon content. Both the amount of coke deposited on the catalysts and the deactivation rate decreased with increasing Mg/Al ratio. This result can be explained in two ways. One is the Ni particle size and the other is the role of the $NiAl_2O_4$ phase. As reported previously, carbon deposition on the catalyst takes place by the consecutive dissociation of CH_4 over the reduced Ni metal, which is the active site for the partial oxidation of CH_4. Therefore, a large Ni metal particle dissociates the CH_4 molecules more rapidly and will be deactivated sooner.

Table 4
Degree of deactivation: effects of calcination temperature.

	NiHT(5) c(623)	NiHT(5) c(773)	NiHT(5) c(923)	NiHT(5) c(1073)
Initial activity (%)	76.79	78.22	79.27	78.90
Deactivation factor [a]	0.92	0.96	0.97	1.00

[a] Defined as the ratio of activity after 10 h reaction/initial activity.

As shown in the XRD results in table 2, the NiO particle size decreased with increasing Mg/Al ratio, which is due to an increase in the crystallinity of the synthesized Ni–Mg/Al LDHs. The LDHs have an optimum M^{2+}/M^{3+} ratio of approximately 3. Therefore, the amount of isolated species is minimized at this point. It is likely that the smaller the Ni particle size, the more the rapid dissociation of CH_4 is suppressed. Thus the resistance to carbon deposition is enhanced.

NiHT(0)c(1073) showed a structure similar to that of pure $NiAl_2O_4$. The NiO phase content increased with increasing Mg/Al ratio. However, most of the NiO phase in the catalysts was not reducible until the neighboring $NiAl_2O_4$ began to be reduced. As shown in figure 7, under the reducing conditions used in these experiments, the catalysts were partially reduced NiO–$NiAl_2O_4$. In order to elucidate the role of $NiAl_2O_4$, Ni–Mg/Al oxide catalysts calcined at various temperatures were adapted to the partial oxidation of CH_4. Table 4 summarizes the results from the NiHT(5) catalysts calcined at between 623 and 1073 K. From these results, it was found that the calcination temperature did not seriously affect the initial activity of the catalysts. However, the deactivation rate was much higher in the samples calcined at lower temperatures. This suggests that the Ni metal, which is surrounded by an $NiAl_2O_4$ local order, is the active component in

Table 3
Degree of deactivation and carbon amount of catalysts after 10 h reaction.

	NiHT(0) c(1073)	NiHT(0.5) c(1073)	NiHT(2) c(1073)	NiHT(5) c(1073)	NiHT(∞) c(1073)
Deactivation factor [a]	0.98	0.97	0.98	1.00	0.54
Carbon amount after 10 h reaction (wt%)	0.57	0.70	0.49	0.28	0.75

[a] Defined as the ratio of activity after 10 h reaction/initial activity.

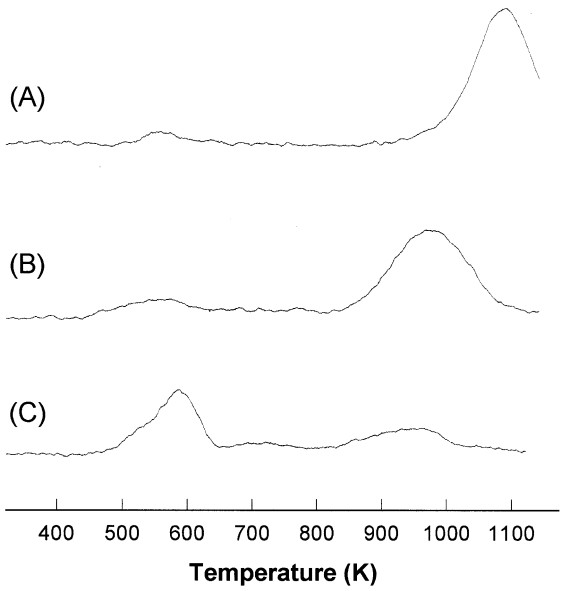

Figure 8. TPR profiles of (A) NiHT(5)c(1073), (B) NiHT(5)c(773), (C) NiHT(5)c(623).

the partial oxidation of CH_4 and this component has a strong resistance to carbon deposition. UV-DRS analysis on the catalysts calcined at 623 K (not shown) indicated that the $NiAl_2O_4$ phase coexisted with the NiO phase. Figure 8 shows the TPR results of the NiHT(5) catalysts calcined at 623, 773 and 1073 K. As the calcination temperature increased, the peak at the lower temperature (for NiO) became smaller and the peak at the higher temperature (for $NiO + NiAl_2O_4$) shifted to a higher temperature. The NiO particle size increased with increasing calcination temperature. Therefore, the fact that those catalysts calcined at higher temperatures showed better activities means that the $NiAl_2O_4$ phase has a positive role in their resistibility against carbon deposition. Recent papers have suggested the presence of a porous nickel aluminate shell surrounding the metallic nickel under reduced conditions [16,17]. In this model, Ni particles are not tightly encapsulated but exhibit voids and pores. This guarantees access for small molecules through the aluminate shell [18]. Therefore, it is likely that the partially reduced $NiAl_2O_4$ phase itself is an active site for the partial oxidation of CH_4 and that it also keeps the neighboring NiO phase from excessive CH_4 dissociation. In order to confirm the above role of the $NiAl_2O_4$ phase, the CH_4 dissociation experiments were carried out using the same procedure as for the partial oxidation of CH_4, except that only CH_4 was used as the reactant. The results showed that the conversion of CH_4 after a 1 h reaction were 6.6 and 4.5% for NiHT(5)c(773) and NiHT(5)c(1073), respectively. This lower dissociation rate of CH_4 over a catalyst calcined at higher temperature supports the above-mentioned role of $NiAl_2O_4$.

4. Conclusions

The catalytic partial oxidation of CH_4 to syngas was carried out over Ni–Mg/Al mixed-oxide catalysts prepared from LDH-type precursors. The NiHT(0)c(1073) catalyst showed a structure similar to that of pure $NiAl_2O_4$, while the other catalysts had a mixed $NiO–NiAl_2O_4$ structure. However, most of the NiO phase in these catalysts was not reduced until the reduction temperature of $NiAl_2O_4$ was reached, indicating that the reduction of the NiO phase was hindered by the $NiAl_2O_4$ phase. In the catalytic reaction, CH_4 was converted into syngas with a 90% or higher selectivity. The NiHT(∞) catalyst did not have an LDH structure and had a poor activity. The NiHT(5)c(1073) catalyst, prepared from highly crystalline LDH precursors, showed the best activity and resistance to carbon deposition. This can be explained by two facts. One is the smaller Ni particle size due to this high crystallinity, and the other is the presence of an $NiAl_2O_4$ spinel phase, which plays a positive role in resisting coke formation. TPR and UV-DRS revealed that the $NiAl_2O_4$ phase was already formed by calcination at lower temperatures. As the calcination temperature increased, the CH_4 dissociation rate decreased and the reaction stability was enhanced. $NiAl_2O_4$ was found to be responsible for this catalyst stability, leading to a low catalyst deactivation rate.

References

[1] V.R. Choudhary, A.M. Rajput and B. Prabhakar, Catal. Lett. 32 (1995).
[2] A.T. Ashcroft, A.K. Cheetham, J.S. Foord, M.L.H. Green, C.P. Grey, A.J. Murreill and P.D.F. Vernon, Nature 344 (1990) 319.
[3] D. Dissanayake, M.P. Rosynek, K.C.C. Kharas and J.H. Lunsford, J. Catal. 132 (1991) 117.
[4] T. Hayakawa, A.G. Anderson, M. Shimizu, K. Suzuki and K. Takehira, Catal. Lett. 22 (1993) 307.
[5] P.M. Torniainen, X. Chu and L.D. Schmidt, J. Catal. 146 (1994) 1.
[6] L. Cao, Y. Chen and W. Li, Stud. Surf. Sci. Catal. 107 (1997) 467.
[7] F. Basile, L. Basini, M. D'Amore, G. Fornasari, A. Guarinoni, D. Matteuzzi, G. Del Piero, F. Trifiro and A. Vaccari, J. Catal. 173 (1998) 247.
[8] E.C. Kruissink, L.L. van Reijen and J.R.H. Ross, J. Chem. Soc. Faraday Trans. 177 (1981) 649.
[9] F. Arena, A. Parmaliana, N. Mondello, F. Frusteri and N. Giordano, Langmuir 7 (1991) 1555.
[10] V.R. Choudhary and A.S. Mamman, Appl. Energy 66 (2000) 161.
[11] M.V. Twigg and J.T. Richardson, Appl. Catal. A 190 (2000) 61.
[12] J.R.H. Ross and M.C.F. Steel, J. Chem. Soc. Faraday Trans. 69 (1973) 10.
[13] J. Zielinski, Catal. Lett. 12 (1992) 389.
[14] M. Jitianu, A. Jitianu, M. Zaharescu, D. Crisan and R. Marchidan, Vibrat. Spectrosc. 22 (2000) 75.
[15] R. Jin, Y. Chen, W. Li, W. Cui, Y. Ji, C. Yu and Y. Jiang, Appl. Catal. A 201 (2000) 71.
[16] J. Zielinski, Appl. Catal. A 94 (1993) 107.
[17] R. Lamber and G. Schulz-Ekloff, J. Catal. 146 (601) 1994.
[18] F. Medina, P. Salagre, J.L.G. Fierro and J.E. Sueiras, J. Chem. Soc. Faraday Trans. 89(18) (1993) 3507.